Multiscale Damage Modelling of Sustainable Composites

Shyam M. Panamoottil[1], †* Raj Das[2], and Krishnan Jayaraman[1]

[1]Department of Mechanical Engineering, University of Auckland, New Zealand
[2]School of Engineering, RMIT University, Australia

*Presenting author: raj.das@rmit.edu.au
†Corresponding author: raj.das@rmit.edu.au

Abstract

A computational homogenization technique has been implemented using the ABAQUS finite element solver to analyse the behaviour of flax fibre composites subjected to three-point bending. Macroscale models of bending specimens were coupled with numerically estimated damage rules for two systems each of flax/polypropylene and flax/epoxy. The results obtained for the failure strength were between 7.5-11.2% lower than the test average values. Validation studies were also performed, using geometry and material parameters for a glass/epoxy composite, and the predicted failure strength was only 12.6% lower than the experimental average for the glass/epoxy three-point bending specimens.

Keywords: Multiscale, Homogenization, Damage, Sustainability, Flax, Composites.

Introduction

Composites can be manufactured in a range of different configurations, using short or long fibres, which are present in either random or oriented manner in the matrix material. For higher performance applications, it is common to utilise long fibres, which can be obtained in fabric form. Shown in Figure 1 are the various stages of producing a composite from fabric. Yarns are composed of several fibres twisted together (Figure 1), which are then woven to produce fabrics (Figure 1). Layers of fabric are then stacked together and infused with matrix/resin to form a composite. As shown in the illustration (Figure 1), the multiscale structure of composites materials results in the response to loading being contributed to by components at different length scales.

(a) (b)

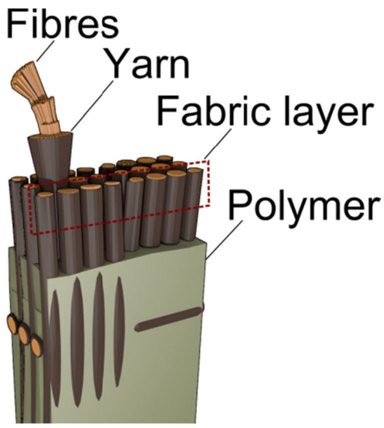

(c)

Figure 1. Illustration of a composite made from yarn fabric - (a) yarn composed of twisted fibres, (b) fabric from yarn, (c) stack of fabric layers and (d) fabric stack infused with resin

The heterogeneous and multiscale nature of composite materials causes them to demonstrate failure behaviour that is quite different from that of metals or other materials which might have been traditionally used in certain applications. The various failure processes observed could include fibre fracture and interface failure at the fibre-interface scale [1] (microscale), matrix cracking and delamination at the yarn-lamina scale (mesoscale) [2]. Local damages/cracks interact with each other, sometimes synergistically, and finally may lead to catastrophic failure [3] at the composite level. Macroscale damage may present as longitudinal splitting, shear crippling or complete rupture, among other modes. Local phenomena thus indirectly dictate the final failure properties of composites.

Due to the complexity involved in composite failure, coupled multiscale modelling techniques are necessary to capture the failure mechanisms at the different geometric scales [4, 5]. Such techniques typically couple local analysis of RVE models with global or macro analysis [6-8]. Most of these techniques can be classified as superposition techniques [9-15] mathematical homogenization techniques [16-21], domain decomposition techniques [22-26] and multiscale computational techniques [8, 27-30]. Among the various techniques explored, the approach taken by Smit et al. [8, 29, 31] is to be noted for being *non-intrusive*, meaning that it can be easily implemented with commercial finite element (FE) codes.

Natural fibre composites (NFCs) are also increasingly being adopted [32, 33] in the automobile and construction industries worldwide. The NATEX (Aligned Natural Fibres and Textiles for Use in Structural Composite Applications) project [34] funded by the European Union was a recent example of an effort to progress the knowledge on bio-based resins and natural fibre fabric precursors. Coordinated efforts were made by research centres and commercial institutions spread across several countries to develop materials and manufacturing techniques for NFCs which could be readily adopted by commercial operations for structural applications. In this context, NFCs are ideal candidates for application of multiscale techniques to predict mechanical properties, so that greater confidence in their application in structures can be established.

This paper explores the application of the computational homogenization technique of Smit et al. [35-37] to predict the behaviour of flax fabric composites subjected to three point bending. Panels of four different flax-based material systems will be manufactured, and their bending behaviour determined through tests on specimens from the panels.

Materials and Methods

In this work, we reinforced a thermoplastic polymer and a thermoset polymer separately with continuous flax fibre reinforcement . For the thermoplastic, Polypropylene (PP) (Moplen RP241G, Lyondell Basell, New Zealand) was obtained in the form of 0.38 mm and 0.6 mm sheets. Prime 20 LV, Gurit, New Zealand was used for the thermoset composites. The matrix polymers properties are listed in Table 1. Unidirectional flax fibre fabric (Belgian flax, *linum usitassimum*) of areal density 190 g/m^2 was obtained from Libeco, Belgium.

Glass/epoxy composites were also manufactured and tested to validate some of the numerical models. Glass unidirectional (UD) fabric of areal density 250 g/m^2 obtained from Gurit, New Zealand was used to manufacture these composite panels.

Table 1. Properties of the matrix polymers.

Material	Property	Value
PP	Density	0.9 g/cm3
	Tensile modulus, E	1.1 GPa
	Yield strength, σ_y	10 MPa
Epoxy (Prime 20 LV)	Density	1.089 g/cm3
	Tensile modulus, E	3.2 GPa
	Yield strength, σ_y	73 MPa

Manufacture

Flax/PP panels of two volume fractions, 0.22 and 0.41 were manufactured using a 100 tonne press. PP sheets and layers of flax fabric were assembled and compacted in a die which was pre-heated to 190 °C. A pressure of 0.5 MPa was applied for 10 minutes initially, which was then increased to 0.94 MPa over 5 minutes. The die was then cooled to 100 $^{\circ}$C, maintaining the pressure at 0.94 MPa.

The vacuum-assisted resin transfer moulding (VARTM) process was used to manufacture the flax/epoxy panels of two different volume fractions, 0.41 and 0.51, and glass/epoxy panels of volume fraction 0.51. The mould was heated prior to placing the fabric inside. On completing injection, the mould was heated to 60○C to ensure complete curing of the resin.

For further details of both manufacturing processes, the authors' earlier paper can be referred to [35]. Designations have been assigned to the composite materials for ease of reference. The flax/PP composites with 0.22 and 0.41 volume fractions will be referred to as FLPP22 and FLPP41 respectively. Similarly, the flax/epoxy systems composites with 0.41 and 0.51 volume fractions will be referred to as FLEP41 and FLEP51 respectively, and the glass/epoxy system as GLEP51.

Mechanical tests and analysis

Three-point bending tests were performed to study the macroscale behaviour of the composite materials, following the ASTM D790 standard. Rectangular specimens 84 mm long by 16 mm wide for three-point bend (flexural) tests were extracted from the panels produced. As per the ASTM D790 standard, the strain rate applied to flexure specimens was decided based on initial testing done on a sacrificial specimen. The support span and strain rates for all material systems were calculated from the dimensions of this specimen, as per the procedure specified in the standard, and these values are listed in Table 2.

Table 2. Parameters used for three point bend/flexure tests on composite specimens

Material system	V_f	Designation	Support span [mm]	Strain rate [mm/min]
Flax/PP	0.22	FLPP22	47.85	1.315
Flax/PP	0.41	FLPP41	47.85	1.315
Flax/epoxy	0.41	FLEP41	63.74	1.737
Flax/epoxy	0.51	FLEP51	63.74	1.750
Glass/epoxy	0.51	GLEP51	63.64	1.728

As part of a previous study [35], we also characterized mechanical properties at the microscale. The strength of flax fibres under tension was determined using single fibre tensile tests (SFTTs) performed according to the ASTM C1557 standard, with specimens of four different gauge lengths of 10, 15, 20 and 25 mm being tested. The normal strength of the interface between fibres and matrix polymer was also studied for flax/PP and flax/epoxy using the microbond technique. Transverse tensile strength of composites was determined following the ASTM D3039 standard to estimate the shear strength of the fibre-matrix interface.

Macroscale properties

Tensile testing of rectangular specimens was performed using a 30 kN Instron 5567 UTM with a video extensometer to measure strain. As per the ASTM D3039 standard, testing was performed at a crosshead rate of 2 mm/min. Compressive tests were performed either using the Instron 5567 UTM or a 100 kN Instron UTM depending on the final load required for the material system. The ASTM D6641 standard using a combined loading fixture was employed, and the test was performed at a crosshead speed of 1.3 mm/min. Rail shear specimens were tested as per the ASTM D4255 standard. Composite specimens were also tested in flexure by performing three-point bending tests following the ASTM D790 standard.

Fabric geometry characterization

A Leica MZ16 microscope with a maximum magnification of 220x was used for optical microscopy measurements. Various optical measurements, such as the centre-to-centre distance between individual warp yarns and individual weft yarns, were performed on the fabrics. These parameters are required for the modelling of the yarn paths, crossovers and spacings, which constitute the architecture of the fabric. For the warp yarns, the distributions of yarn heights and yarn widths were measured for suitability of fitting to normal, log-normal and Gumbel distributions. The fabric geometry distributions were applied to construct the geometric model of the flax fabric using varying yarn geometries [36].

Numerical Modelling

The approach taken to implement the multiscale coupling for this study is illustrated in the flowchart (Figure 2), including the models involved and the exchange of information between them.

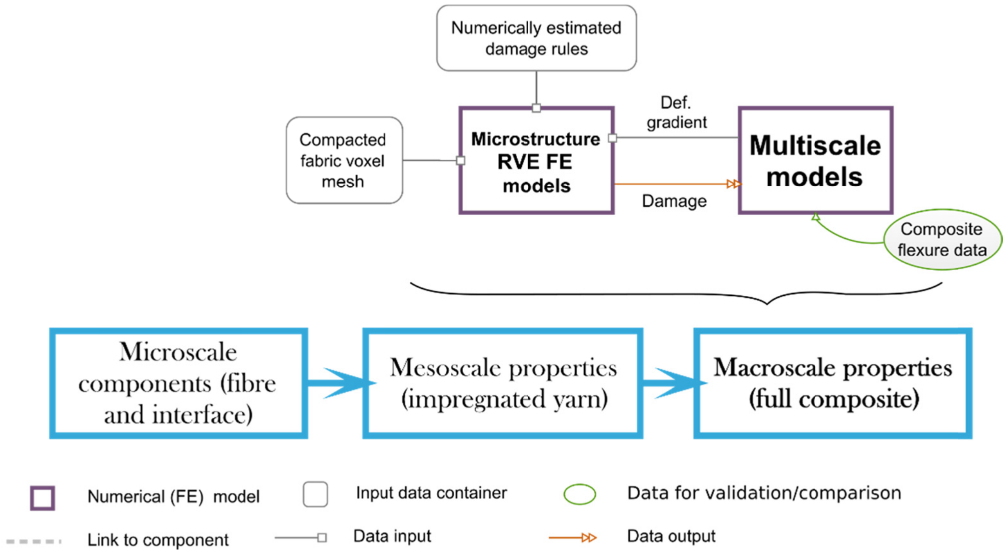

Figure 2. Data exchange involved in the multiscale FE framework

Macroscale model of three-point bending

The multiscale coupling in this study was used to analyse the behaviour of flax composite specimens under three-point bending. As shown in Figure 3, the three-point bending (TPB) test consisted of a rectangular specimen balanced on top of two steel rollers, and a loading roller bending the specimen by pushing down its middle section. The test configuration was represented by a half-symmetry model with solid elements for the beam, and analytical rigid parts representing the loading and support rollers (Figure 3). The ABAQUS CAE python scripting interface was used to parametrically generate the models for the different material systems, and the *getInputs* command enabled the collection of the geometry, material and boundary condition parameters.

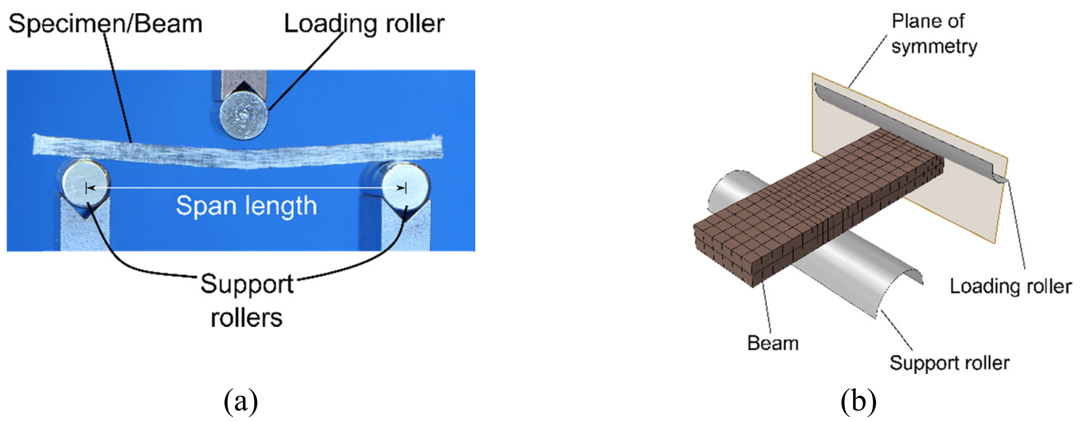

Figure 3. (a) Configuration of the three-point bending test, and (b) representation of the geometry in the FE model of the system

The rollers were positioned so as to replicate the span length used for the particular material system (Table 2). Contact definitions were made between each roller and the beam, and increased mesh refinement was used in areas of the beam closer to the rollers (Figure 3). An initial step was created, displacing the support roller upwards by a small displacement of 10^{-3} mm to establish contact with the beam. In the subsequent step, the loading roller was displaced downwards to deflect the beam.

Microstructure RVE FE models

In a previous study [36], we established a methodology to estimate the damage evolution behaviour in flax/PP and flax/epoxy systems using numerical representative volume element (RVE) models of flax yarns impregnated with either PP or epoxy. The damage rules obtained from these models were then combined with *meso-FE models* [37], which would then be able to provide the macroscale models with a damage response given the deformation gradient. The meso-FE models in this case had discrete representation of the fabric geometry in the flax fabric composites. These are the models referred to as "Microstructure RVE FE models" in Figure 2. The damage rules which were estimated flax/PP and flax/epoxy systems are as in Table 3.

Table 3. Polynomial fit parameters for numerical damage evolution

Material system	**Initial strain**	**a_0**	**a_1**	**a_2**	**a_3**
Flax/PP					
d11	0.0	0.0466	-11.326	6899.025	-177591.065
d22	0.002	0.1594	-84.802	21261.602	-1007230.523
d33	0.002	0.1594	-83.350	20546.880	-986335.330
d12	0.002	0.1592	-84.657	21233.65	-1005611.546
d13	0.0	0.04	-0.581	5227.291	-111522.741
d23	0.002	0.1594	-84.807	21262.992	-1007340.688
Flax/epoxy					
d11	0.008	3.950	-1148.067	104071.570	2752583.210
d22	0.0065	0.0627	-14.474	670.675	18751.528
d33	0.0065	0.0672	-15.484	731.900	17979.630
d12	0.0065	0.072	-13.301	207.513	41757.377
d13	0.01	2.644	-578.704	39704.457	-803754.974
d23	0.0065	0.091	-21.596	1217.099	5652.155

An example of flax composite geometry in the RVEs is shown in Figure 4. From the compacted geometry representing stacks of flax fabrics (Figure 4), FE models were generated with elements filling in spaces between the fabric layers to represent the polymer resin (Figure 4).

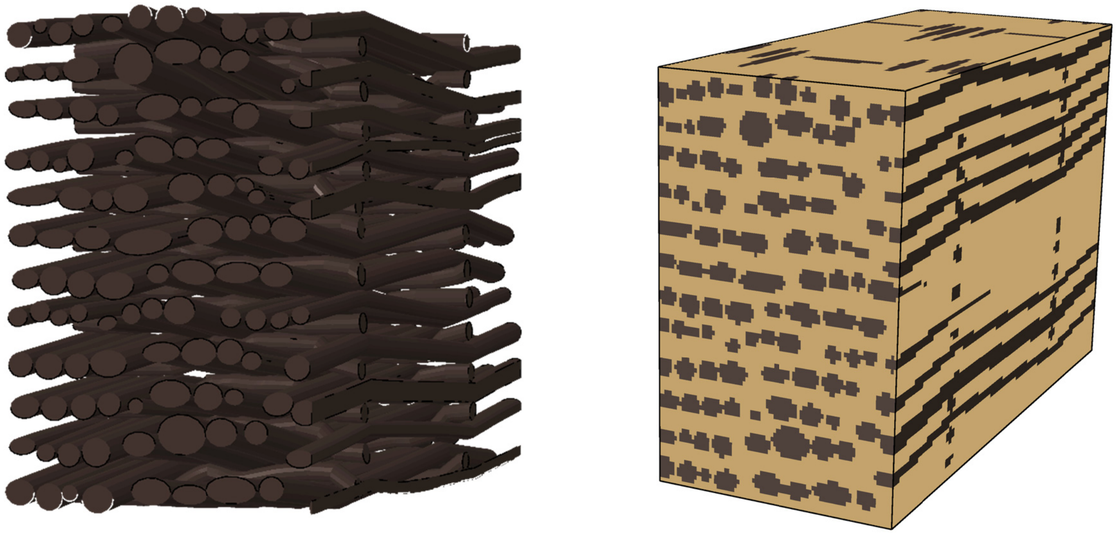

(a) (b)

Figure 4. Illustration of (a) section of compacted fabric geometry and (b) RVE of flax fabric composite

Multiscale coupling

The coupling of scales was performed using a coupled computational homogenization method [31] because it is relatively easy to implement, and is also non-intrusive. The term "*non-intrusive*" indicates that the method does not require access/modifications to the numerical solver code itself.

In the method, the macroscopic model is solved first, and for each iteration and each integration point in the elements, the macroscopic deformation gradient F_{macro} is obtained. In the ABAQUS UMAT user subroutine, the deformation gradient is stored in the variable DFGRD1. The RVE model displacements were calculated from the deformation gradient using equations of the form

$$[X - x] = [F_{macro} - I].[x] \tag{1}$$

where X and x are the positions of a point in the RVE model in the deformed and original configurations, respectively, and I is the identity matrix. Periodic boundary conditions were imposed on the boundary nodes of the RVE models. Pilot nodes were used to control the boundary nodes, due to which displacements only needed to be specified at the pilot nodes. The RVE model was then solved, followed by volume-averaging of the stress or damage values in the RVE. The damage in the RVE was set by using the numerically estimated strain-damage rules (Table 3). The average values were then updated in the corresponding integration point in the macroscale model. The flow of data between the macroscopic and microscopic meshes is illustrated in Figure 5.

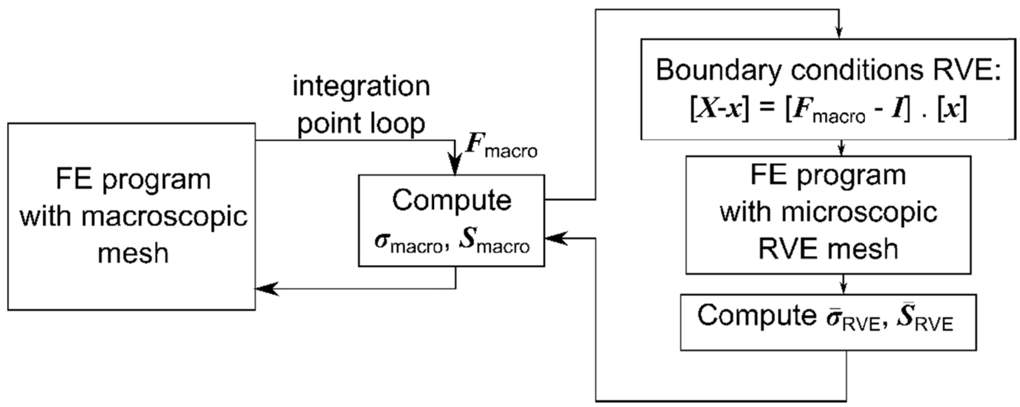

Figure 5. Flowchart of steps involved in the computational homogenization scheme of Smit et al. [31]

The macroscopic meshes used as part of the multiscale coupling in this work were from the FE models representing the three-point bending test (Figure 3). The composite beams were modelled as rectangular blocks with isotropic material properties in these. The microscopic or lower scale models were comprised of the meso-FE RVE models.

Results and Discussion

A hierarchical approach was applied, which includes obtaining material properties at the micro-scale, linking them to analytical or numerical models, and then feeding the micro-scale properties into a larger scale model. Fibre properties were determined first, fit to Weibull distributions, and compared to predictions using the classical laminate theory. The fibre properties were then used in simulations of the microbond test performed to determine properties of the interface. The properties of the fibre and the interface were subsequently used to model the failure of matrix-impregnated flax yarns.

Fabric geometry characterization

The measurements of the cross-sections of flax fibres and flax yarns are indicated as distributions in Figure 6. Concerning the flax fabrics, the term "crossover" will from now on mean when a warp yarn passes over a weft yarn or vice-versa. On observation of the fabrics, it was found that the average distance from the edge of one warp flax yarn to the next was 0.005 mm (within the same crossover), while the corresponding value for weft yarns was 2.85 mm. For the glass fabric, the glass tows were closely spaced, and were 2.08 mm wide and 0.24 mm high on average. The tows were bound by polyethylene yarns 0.3 mm wide and 0.2 mm high, which were spaced 37 mm apart.

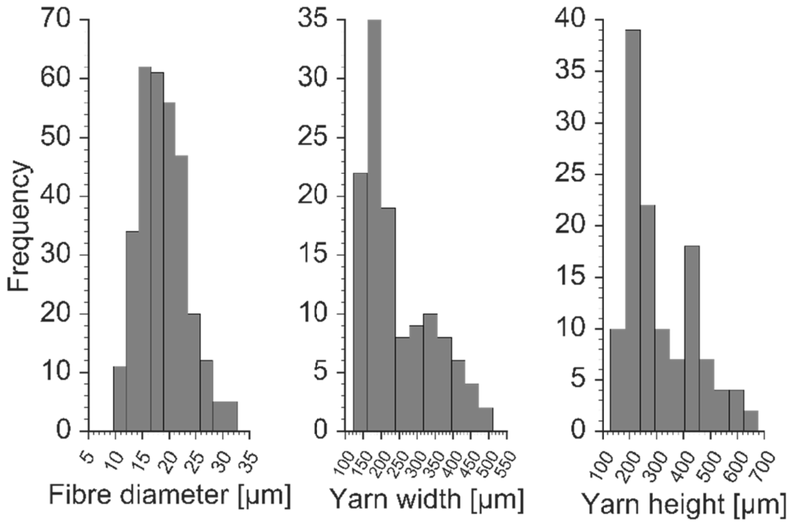

Figure 6. Distributions of fibre and yarn geometries, from optical measurements

Multiscale model results

The simulation results, presented in Figure 7, display reasonably good agreement with the experimental data for all four systems. For the flax/PP systems, the predicted stresses at failure matched closely with those obtained from the tests. For the FLPP22 model, with the numerical damage rule applied, the predicted failure was at 103.10 MPa, which is 8.3% lower than the average experimental value of 112.40 MPa. However, the failure does seem to occur early, with the failure strain of 0.028 being less than half the average strain of 0.060 in the tests. The higher failure strain in the test specimens could be due to the unwinding of the fibres in the yarn helix, and of the cellulose microfibrils in the fibres. Fractographic analysis could confirm the occurrence of such a process. However, fractographic analysis of micromechanics is not a focus of this thesis, and is something that could be investigated as part of another research work.

The prediction for FLPP41 was at a value of 115.78 MPa, which is 7.7% lower than the test value. The failure strain of 0.027 was again lower than the average strain of 0.050 in the tests. Both the stress and strain behaviours predictions were much closer to the average experimental values for the flax/epoxy systems. In the case of the FLEP41 model, the predicted strength was 236.36 MPa, 11.2% lower than the experimental average of 296.40 MPa, while for the FLEP51 model, the strength was predicted to be 299.14 MPa, only 7.5% lower than the test average of 323.4 MPa. The corresponding failure strain prediction of 0.032 was only 7.4% lower than the test average strain of 0.030.

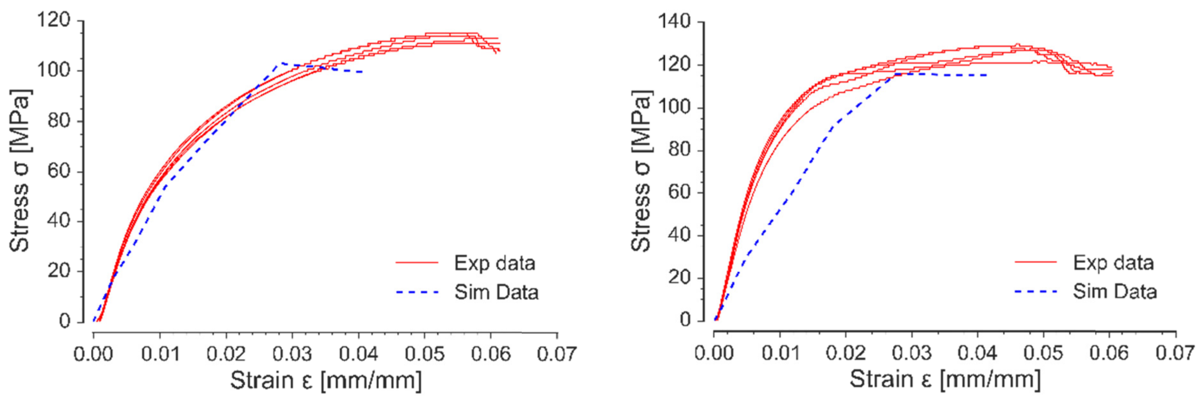

(a) (b)

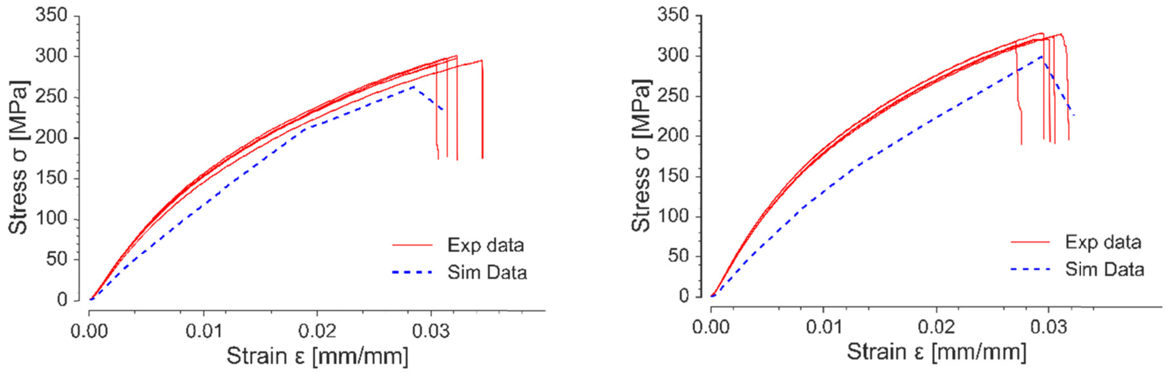

(c) (d)

Figure 7. Results from multiscale simulations of three-point bending behaviour of (a) FLPP22, (b) FLPP41, (c) FLEP41 and (d) FLEP51

Validation with Experiments

The multiscale modelling framework here was demonstrated to yield good results for the four flax composite systems studied. To ascertain the applicability of this method to other material systems, the entire set of experiments and simulations leading up to the multiscale simulations has been repeated for a glass/epoxy material system (GLEP51). Glass/epoxy panels with a fibre volume fraction of 0.51 were manufactured using resin transfer moulding, as mentioned before and subjected to three-point bending tests.

Impregnated yarn RVE and damage rule

Using a similar method as described in our previous paper [36] to establish damage evolution rules for fabric composite systems, discrete models of glass tows impregnated by epoxy resin were constructed and samples cut out to identify RVEs. Damage was calculated based on the values of strain with respect to strain values expected at the plastic yield point of the epoxy and glass fabric. The strength values used for the glass fabric were [38]:

- Longitudinal tensile strength = 2000 MPa
- Longitudinal compressive strength = 1000 MPa
- Transverse tensile strength = 80 MPa
- Transverse compressive strength = 250 MPa
- Shear strength = 100 MPa

The strength used to calculate the yield strain for epoxy was 73 MPa (Table 1). The damage evolution from tensile and compressive loading of the glass/epoxy RVE model were calculated, and best-fits for their evolution obtained by curve-fitting. The parameters for the curves thus obtained for the evolution of damage in the glass elements are specified in Table 4.

Table 4. Polynomial fit parameters for numerical damage evolution of glass/epoxy impregnated yarn

Damage variable	Start strain	a_0	a_1	a_2	a_3
Tensile					
d11	0.005	-1.386	365.707	-19,101.067	333,478.08
d22	0.005	-1.080	284.011	-14,597.98	248,129.125
d33	0.005	-1.077	283.139	-14,553.156	247,367.21
d12	0.002	0.149	-81.43	19,771.52	-865,447.951
d13	0.002	0.153	-86.178	20,474.23	-904,093.44
d23	0.002	0.148	-83.358	18,810.508	-796,770.62
Compressive					
d11	0.0	0.043	-39.310	3,324.354	1,196,582.368
d22	0.0	0.106	-5.213	1,040.962	956,921.524
d33	0.0	0.105	-3.460	1,163.322	908,359.764
d12	0.0	0.110	-5.382	1,074.801	988,028.244
d13	0.0	0.038	-40.331	3,855.576	1,052,958.606
d23	0.0	-0.009	25.622	-2,732.963	1,046,119.704

Multiscale three-point bending

A meso-FE model was constructed for the GLEP51 system using the same methodology utilized to construct meso-FE models for the flax-based systems [37], and the geometry parameters obtained for the glass fabric. The uncompacted and compacted glass fabric geometries used in generating the meso-FE models are shown in Figure 8.

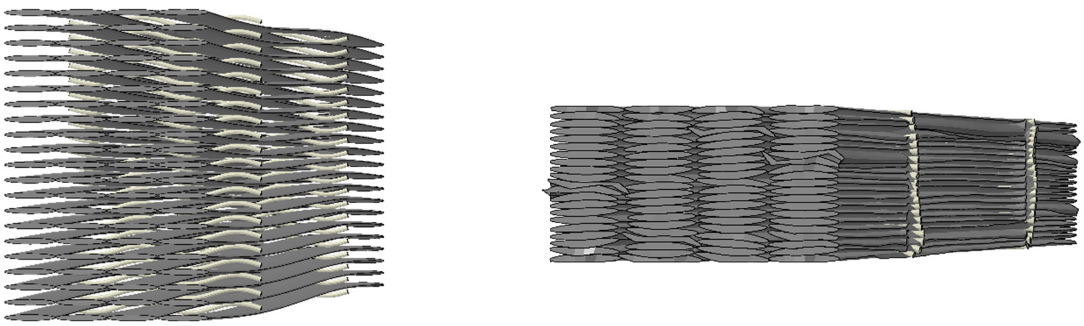

(a) (b)

Figure 8. Glass fabric stack (a) before and (b) after compaction

A model representing the three-point bending of glass/epoxy specimens was constructed, with the initial elastic stiffness of the glass/epoxy composite set to 42.58 GPa. Subsequently, coupled multiscale studies were undertaken to simulate the three-point bending behaviour of GLEP51 models. The bending model was coupled with the meso-FE RVE model for glass/epoxy using FORTRAN code and the UMAT interface in ABAQUS. The bending behaviour predicted by the model was close to the experimental results in terms of the stiffness behaviour and the failure strength value, as shown in Figure 9. The failure was predicted at 898.26 MPa, which is only 12.6% lower than the test average of 1028.17 MPa.

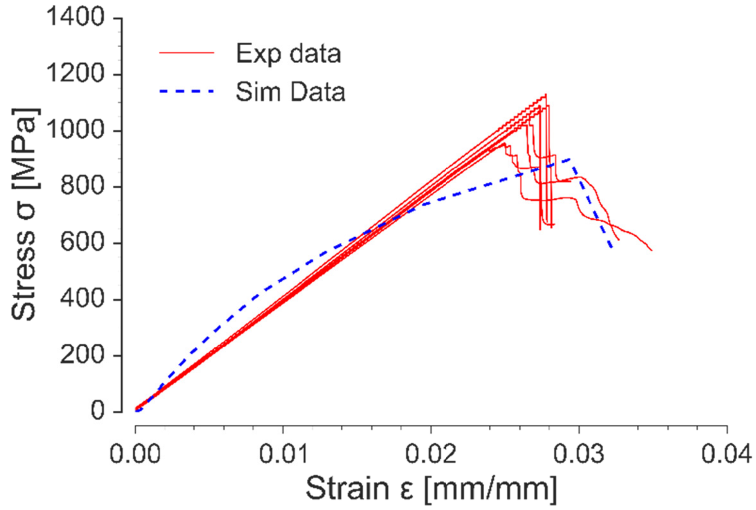

Figure 9. Stress-strain response from the multiscale simulation of three-point bending behaviour of GLEP51, compared to bending test data

Conclusions

A coupled multiscale homogenization technique was implemented to analyze the mechanical behaviour of flax/PP and flax/epoxy fabric composites using ABAQUS and FORTRAN code. Two scales were considered, one of which was an FE representation of a three-point bending specimen. The coupled microscopic meshes or lower scale models were FE models containing discrete representations of the fabric geometry. The failure of the impregnated yarn elements in the lower scale models was implemented using strain-damage evolution laws estimated numerically from the fibre and interface properties. The implementation was used to simulate the bending behaviour of the composites. The results obtained for the failure strength were between 7.5-11.2% lower than the test average values.

Validation studies for the technique were also performed, using geometry and material parameters for a glass/epoxy composite, combined with flexure test data. Numerical damage evolution laws were obtained for the glass/epoxy system. The coupled homogenization technique was then applied to the glass/epoxy system, as performed for the flax composites. The stiffness and strength behaviours were reasonably close to those of the test specimens, and the predicted failure strength was only 12.6% lower than the experimental average for the glass/epoxy three-point bending specimens.

Finite element models containing discrete representations of the fabric geometry (meso-FE models) can be used to predict the tensile failure of natural fibre composites, as demonstrated using flax fibre-based composites. This was demonstrated for four flax/polymer composite systems by combining the fabric geometry with the strain-damage evolution rules. These rules were obtained by constructing FE models from cuboid samples extracted from the impregnated yarn geometry. Equipped with the fibre, interface and matrix polymer properties, damage evolution laws can be obtained for any fibre-polymer combination by following the approach in this work.

The present work establishes the reliability in applying numerical damage rules for multiscale modelling of natural fibre-based composites. To do so, a coupled multiscale homogenisation technique was implemented to establish its capability to predict the mechanical behaviour of natural fibre thermoplastic and thermoset composite materials. This has been demonstrated by applying the multiscale model to the bending analysis two flax/PP and two flax/epoxy composite systems, with reasonably accurate results obtained. The multiscale framework was two-scale, consisting of a homogenised material model at the highest level coupled with a microstructure model. A validation study was performed to establish the reliability of the same framework using a glass/epoxy composite material system, which was also able to predict the composite failure with good accuracy. Overall, these sets of results establish the confidence in the potential of this multiscale framework implementation in relation to its applicability for different composite material systems.

Acknowledgements

The authors would like to thank the Ministry of Business, Innovation and Employment, New Zealand, for the funding provided to support this project through grant no. 3625485 titled "Sustainable Composites". The authors also wish to acknowledge the contribution of NeSI high-performance computing facilities to the results of this research.

References

[1] Matzenmiller, A., Lubliner, J., and Taylor, R.L. (1995) A constitutive model for anisotropic damage in fiber-composites, *Mechanics of Materials* **20** (2), 125-152.
[2] Nairn, J.A. (2000) 2.12 - Matrix Microcracking in Composites, *Comprehensive Composite Materials*. 403-432.
[3] Talreja, R. (1985) A Continuum Mechanics Characterization of Damage in Composite Materials, *Proceedings of the Royal Society of London. A. Mathematical and Physical Sciences* **399** (1817), 195 -216.
[4] LLorca, J., Gonzalez, C., Molina-Aldareguia, J.M., Segurado, J., Seltzer, R., Sket, F., Rodríguez, M., Sadaba, S., Munoz, R., and Canal, L.P. (2011) Multiscale Modeling of Composite Materials: a Roadmap Towards Virtual Testing, *Advanced Materials*.
[5] Nguyen, B.N., Bapanapalli, S.K., Holbery, J.D., Smith, M.T., Kunc, V., Frame, B.J., Phelps, J.H., and Tucker, C.L. (2008) Fiber Length and Orientation in Long-Fiber Injection-Molded Thermoplastics - Part I: Modeling of Microstructure and Elastic Properties, *Journal of Composite Materials* **42** (10), 1003-1029.
[6] Xiao, Q.Z., and Karihaloo, B.L. (2010) Two-scale asymptotic homogenisation-based finite element analysis of composite materials, *Multiscale Modeling in Solid Mechanics: Computational Approaches*. 43-100.
[7] Llorca, J., González, C., and Segurado, J. (2007) Finite element and homogenisation modelling of materials, *Multiscale materials modelling*. 121-147.
[8] Smit, R.J.M., *Toughness of Heterogeneous Polymeric Systems : A Modeling Approach*, Eindhoven Technical University, 1998.
[9] Noor, A.K. (1986) Global-local methodologies and their application to nonlinear analysis, *Finite Elements in Analysis and Design* **2** (4), 333-346.
[10] Whitcomb, J.D. (1991) Iterative global/local finite element analysis, *Computers & Structures* **40** (4), 1027-1031.
[11] Fish, J., Belsky, V., and Pandheeradi, M. (1996) Composite grid method for hybrid systems, *Computer Methods in Applied Mechanics and Engineering* **135** (3\textendash4), 307-325.
[12] Haidar, K., Dubé, J.F., and Pijaudier-Cabot, G. (2003) Modelling crack propagation in concrete structures with a two scale approach, *International Journal for Numerical and Analytical Methods in Geomechanics* **27** (13), 1187-1205.
[13] Mote, C.D. (1971) Global-local finite element, *International Journal for Numerical Methods in Engineering* **3** (4), 565-574.
[14] McCormick, S., and Thomas, J. (1986) The fast adaptive composite grid (FAC) method for elliptic equations, *Mathematics of Computation* **46** (174), 439-456.
[15] Fish, J., Suvorov, A., and Belsky, V. (1997) Hierarchical composite grid method for global-local analysis of laminated composite shells, *Applied Numerical Mathematics* **23** (2), 241-258.
[16] Fish, J., Shek, K., Pandheeradi, M., and Shephard, M.S. (1997) Computational plasticity for composite structures based on mathematical homogenization: Theory and practice, *Computer Methods in Applied Mechanics and Engineering* **148** (1-2), 53-73.

[17] Feyel, F., and Chaboche, J.-L. (2000) FE2 multiscale approach for modelling the elastoviscoplastic behaviour of long fibre SiC/Ti composite materials, *Computer Methods in Applied Mechanics and Engineering* **183** (3-4), 309-330.
[18] Peng, X., and Cao, J. (2002) A dual homogenization and finite element approach for material characterization of textile composites, *Composites Part B: Engineering* **33** (1), 45-56.
[19] Fang, Z., Sun, W., and Tzeng, J.T. (2004) Asymptotic Homogenization and Numerical Implementation to Predict the Effective Mechanical Properties for Electromagnetic Composite Conductor, *Journal of Composite Materials* **38** (16), 1371-1385.
[20] Ghosh, S., and Mukhopadhyay, S.N. (1993) A material based finite element analysis of heterogeneous media involving Dirichlet tessellations, *Computer Methods in Applied Mechanics and Engineering* **104** (2), 211-247.
[21] Sanchez-Palencia, E. (1987) General introduction to asymptotic methods, *Lecture Notes in Physics*. 121-136.
[22] Bramble, J.H., and Pasciak, J.E. (1990) A domain decomposition technique for Stokes problems, *Applied Numerical Mathematics* **6** (4), 251-261.
[23] Farhat, C., Wilson, E., and Powell, G. (1987) Solution of finite element systems on concurrent processing computers, *Engineering with Computers* **2** (3), 157-165.
[24] Borgers, C. (1989) The Neumann-Dirichlet domain decomposition method with inexact solvers on the subdomains, *Numerische Mathematik* **55** (2), 123-136.
[25] Toselli, A., and Widlund, O. (2005) *Domain decomposition methods: algorithms and theory,* Springer.
[26] Ladeveze, P., Loiseau, O., and Dureisseix, D. (2001) A micro-macro and parallel computational strategy for highly heterogeneous structures, *International Journal for Numerical Methods in Engineering* **52** (1-2), 121-138.
[27] Boso, D.P., Lefik, M., and Schrefler, B.A. (2006) Homogenisation methods for the thermo-mechanical analysis of Nb3Sn strand, *Cryogenics* **46** (7-8), 569-580.
[28] Renard J, M.M. (1987) Etude de l'initiation de l'endommagement dans la matrice d'un materiau composite par une methode d'homogenisation, *Aerosp Sci Technol* **6**, 37-51.
[29] Kouznetsova, V., Geers, M.G.D., and Brekelmans, W.A.M. (2010) Computational homogenization for non-linear heterogeneous solids, *Multiscale Modeling in Solid Mechanics: Computational Approaches*. 1-42.
[30] Carvelli, V., and Poggi, C. (2001) A homogenization procedure for the numerical analysis of woven fabric composites, *Composites Part A: Applied Science and Manufacturing* **32** (10), 1425-1432.
[31] Smit, R.J.M., Brekelmans, W.A.M., and Meijer, H.E.H. (1998) Prediction of the mechanical behavior of nonlinear heterogeneous systems by multi-level finite element modeling, *Computer Methods in Applied Mechanics and Engineering* **155** (1-2), 181-192.
[32] Bismarck, A., Baltazar-Y-Jimenez, A., and Sarikakis, K. (2006) Green Composites as Panacea? Socio-Economic Aspects of Green Materials, *Environment, Development and Sustainability* **8** (3), 445-463.
[33] Suddell, B.C., and Evans, W.J. (2005) Natural Fiber Composites in Automotive Applications in Natural Fibers in Biopolymers & Their BioComposites, *Natural Fibers, Biopolymers, and Biocomposites*. 231-259.
[34] Commission, E.
[35] Panamoottil, S.M., Das, R., and Jayaraman, K. (2016) Towards a multiscale model for flax composites from behaviour of fibre and fibre/polymer interface, *Journal of Composite Materials*.
[36] Panamoottil, S.M., Das, R., and Jayaraman, K. (2016) Experimentally quantified and computational anisotropic damage rules for flax fabric composites, *International Jounal of Damage Mechanics*.
[37] Lomov, S.V., Ivanov, D.S., Verpoest, I., Zako, M., Kurashiki, T., Nakai, H., and Hirosawa, S. (2007) Meso-FE modelling of textile composites: Road map, data flow and algorithms, *Composites Science and Technology* **67** (9), 1870-1891.
[38] Gan, J.M., Modelling the initiation and evolution of damage within GFRP by including real geometric variability. *18th International Conference on Composite Materials,* 21-28 August, Jeju Island, Korea, 2011.